Exploratory Analysis of Surface Winds in the Equatorial Western Pacific and El Niño*

PAO-SHIN CHU, JAMES FREDERICK,** AND ANDREW J. NASH

Department of Meteorology, School of Ocean and Earth Science and Technology, University of Hawaii, Honolulu, Hawaii

(Manuscript received 26 June 1990, in final form 26 April 1991)

ABSTRACT

Exploratory data analysis is used to examine several key characteristics of surface wind along a ship track in the equatorial western Pacific. A month-by-month examination is undertaken, based on daily ship data from a recent 30-year record (1958–87). The characteristics considered here include the expected frequency of occurrence, the intensity, the range of variability, and the extreme value of the wind from the eight-point compass directions. A hodograph and constancy of monthly mean wind vectors are also presented.

Results from the 30-year climatology suggest that the equatorial western Pacific is affected by monsoonal and trade flows from each winter hemisphere and by the eastern Pacific subtropical highs during the transition season (i.e., May). Equatorial westerlies peak in November (20%) and December (18%).

Composite analysis reveals the further influence of the trade flows from the northwest Pacific from January to May, and the Southern Hemisphere influence from June to September during a year when ENSO has occurred. The reliability of the ENSO composite has been tested using a Monte Carlo simulation technique. Westerlies indeed increase their frequency of occurrence from November of the antecedent year to November of the ENSO year. This increase, however, is small relative to the decrease in easterlies in the same period.

Westerly wind events are examined in terms of their duration and timing of occurrence. Westerly wind events with a period of 5-7 days do occur more often than events with a longer duration, but their frequency of occurrence has reduced substantially during El Niño years.

1. Introduction

There has been a growing interest in the relationship between surface wind variations in the equatorial western Pacific (EWP) and El Niño. The dynamics of this relationship lies in oceanic Kelvin waves that are excited by episodic westerly wind bursts in the EWP. Studies show that the first baroclinic mode of the Kelvin waves takes about two to three months to cross the Pacific basin, with higher modes taking a longer time (e.g., Gill 1982). With an eastward advection of warm water associated with the waves and the depressed thermocline as induced by downwelling Kelvin waves, warm surface waters are found subsequently in the equatorial eastern Pacific, downstream from the remote wind-forcing region in the EWP. There is now much empirical evidence to indicate wind-generated Kelvin pulses in the equatorial waveguide (e.g., Lukas et al. 1984; McPhaden et al. 1988).

Luther et al. (1983), Luther and Harrison (1984), and Harrison and Luther (1990) studied in detail the climatological features of surface winds from tropical Pacific islands. However, in their analyses, a large void exists in the data for the area between 5°N–5°S and 130°E–165°E (e.g., Fig. 1 in Harrison and Luther 1990). More recently, Harrison and Giese (1991) categorized westerly bursts as observed along a string of islands near 175°E into four types, but acknowledged that "Our near-date line results may not be typical of regions to either the east or west." In fact, the synoptic-scale, equatorial westerly bursts are mainly confined in the EWP (Keen 1988; Chu 1988; Chu and Frederick 1990). As such, detection of the bursts in the central Pacific or the eastern Pacific is not necessarily guaranteed. May 1986 is a good case. During this month strong westerlies ($\sim$10 m s^{-1}) were reported at Kapingamarangi atoll ($\sim$1°N, 155°E), but only light to moderate easterlies were observed at Tarawa ($\sim$1°N, 173°E), one of the islands used in Harrison and Luther (1990) and Harrison and Giese (1991). It is important to note here that surface wind data along the ship track are the only source of historical observations available west of 175°E.

Concerning the causes of westerly bursts, Chu (1988) and Chu and Frederick (1990) demonstrated that there is a tendency for a rapid pressure increase in the far western equatorial Pacific following a cold surge-like event in higher latitudes. Since the zonal wind accel-

* Contribution Number 2489 From the School of Ocean and Earth Science and Technology, University of Hawaii.

** Present affiliation: National Weather Service, Concordia, Kansas.

Corresponding author address: Dr. Pao-Shin Chu, Dept. of Meteorology, University of Hawaii, 2525 Correa Road (HIG 331), Honolulu, HI 96822.

eration in low latitudes is dynamically governed by the zonal pressure gradient term, the imposed zonal pressure distribution in the EWP thereby induces downgradient flows toward lower pressure in the east, resulting in the westerly acceleration (i.e., wind bursts). The enhanced convection produced by the initial wind bursts may lead to a further strengthening of equatorial westerlies on the west side of the convection.

The aforementioned linkage between cold surges and local pressure increase is based upon only a few cases and more conclusive evidence needs to be established. Conceivably, other factors that may generate westerly bursts in the EWP include tropical cyclones or cyclone pairs symmetric to the equator (e.g., McPhaden et al. 1988; Nitta 1989) and the tropical 30–60-day oscillations (e.g., Madden and Julian 1972). In addition, using the 3-h digital data from the Geostationary Meteorological Satellite, Nakazawa (1988) and Lau et al. (1989) noted that the 30–60-day mode is characterized by super cloud clusters (SCC), and within SCC, individual convective cells tend to propagate westward. New SCCs develop east of dissipating SCC. Hence, westerly bursts are intertwined with SCC in the 30–60-day mode.

Since the bursts are intermittent synoptic-scale phenomena, the monthly averaged wind data often mask the presence of the bursts. As an example, Fig. 1 shows the time series plot of the surface wind at 6-h intervals for October and November 1971 at Kapingamarangi. In Fig. 1a, a westerly burst occurs during the last three days of October 1971, but the averaged wind for this month is mainly easterly with a speed of 2.5 m s^{-1}. This burst continues into the first few days of November 1971 with a speed as strong as 15 m s^{-1} on 4 November (Fig. 1b), and precedes the initial warming in the eastern equatorial Pacific, which occurred around February and March 1972 (Fig. 1c).

Because of the short duration of the burst (i.e., synoptic time scale) that extends from October to November, it is no wonder that sometimes the monthly averaged data, or even the anomalies from the long-term monthly mean, cannot resolve the high-frequency variability of the surface winds. In order to understand the initiation and maintenance of El Niño Southern Oscillation (ENSO) phenomena, daily wind data along the unique ship track in the EWP should be fully explored. This, however, immediately raises the question of how to present the large amount of daily data in terms of a few important and relevant statistics. To overcome this problem, the current study will use an exploratory analysis to illustrate graphically the climatology of daily wind vectors and variations of daily winds during an ENSO cycle.

More specifically, the expected frequency of occurrence of daily wind vectors that are divided into the eight standard compass groupings of 45° each will be quantified, month by month. Among other things, the intensity of the speed (location parameter), the range

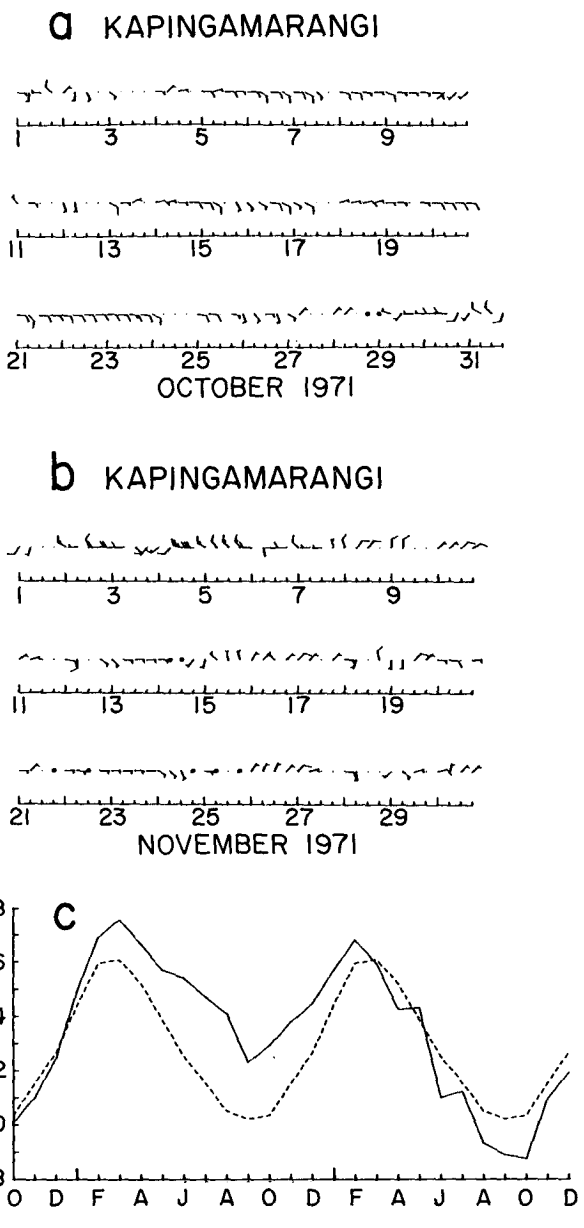

FIG. 1. Time series of surface wind at 6-h intervals for Kapingamarangi for (a) October 1971 and (b) November 1971; (c) time series of monthly median of sea surface temperature (°C) for El Niño regions 1 and 2 (solid) from October 1971 to December 1973. Broken line refers to the climatology for the same area. El Niño regions 1 and 2 cover the area 0°–10°S, 90°–80°W (off the South American coast).

of variability of the speed (scale parameter), and the statistical distribution of the speed for a particular wind direction are examined. Similarly, the wind statistics composited during an ENSO cycle are investigated, and the Monte Carlo sampling technique is used to assess the significance of ENSO composite winds. We will also focus on the statistics of westerly wind events for both climatology and ENSO cycle.

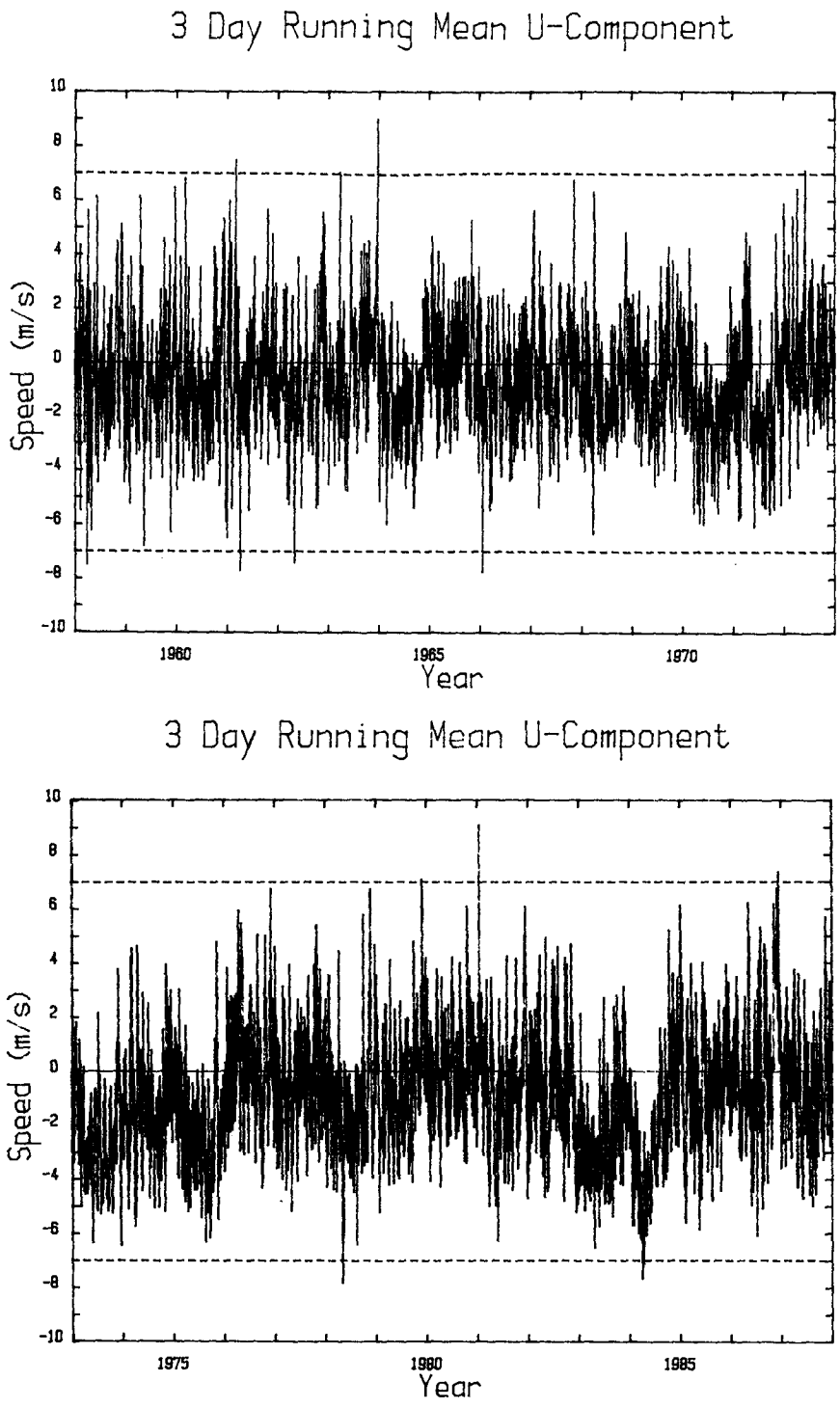

FIG. 2. Time series of the zonal component of the surface wind in the equatorial western Pacific from 1958 through 1987. Three-day running mean is used.

2. Data

Since few islands are located in the EWP, individual marine reports from the shipping lane (i.e., Australia to Japan) will be used. These data come from the Comprehensive Ocean–Atmosphere Data Set (COADS) and the interim COADS, produced by the Environmental Research Laboratory of National Oceanic and Atmospheric Administration in Boulder, Colorado. Surface wind reports from all available ship

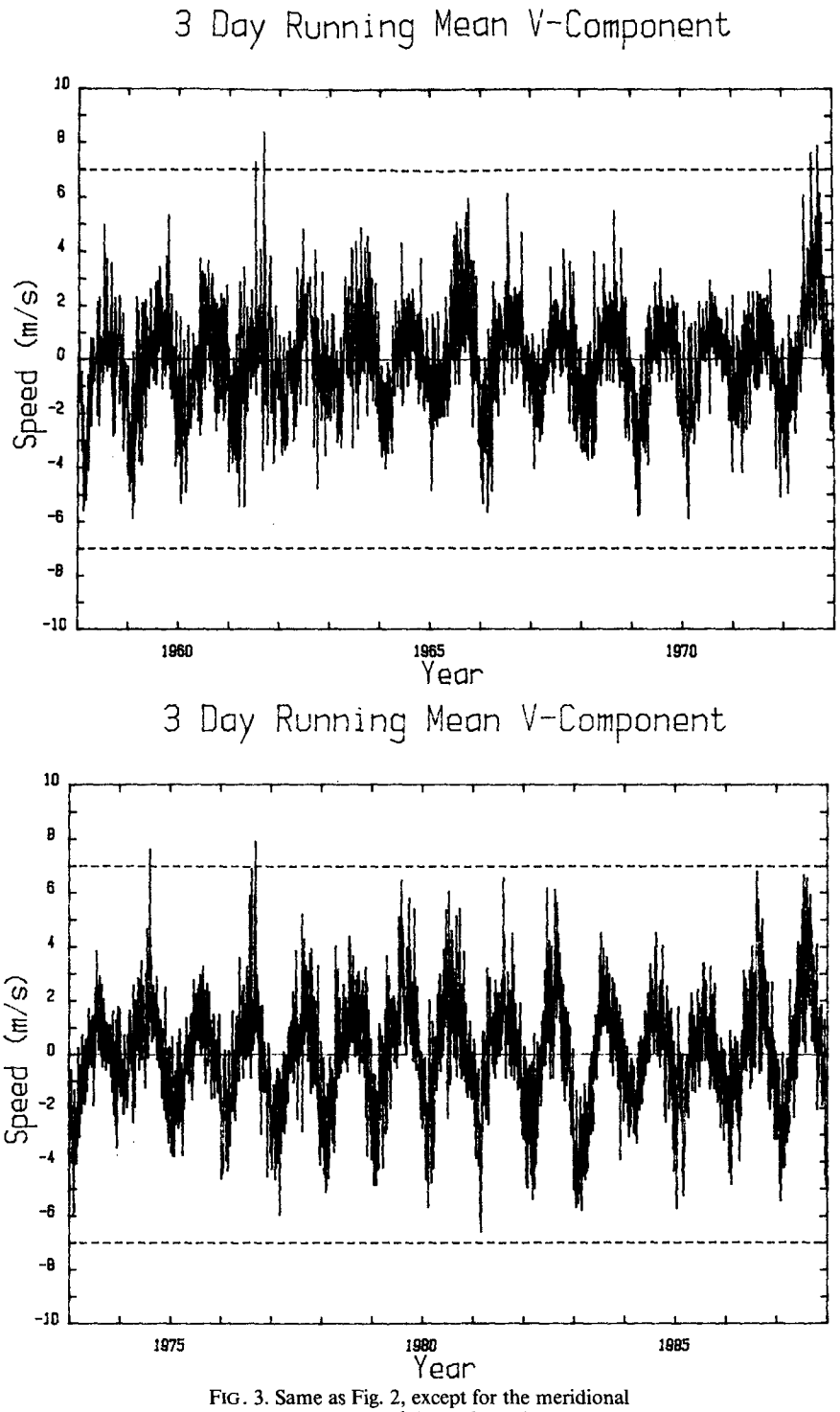

FIG. 3. Same as Fig. 2, except for the meridional component of the surface wind.

observations in the box bounded by 5°N–5°S, 140°E–160°E are averaged to produce daily mean values. In fact, this is the only region in the EWP where the density of ship observations is suitable for statistical analyses (e.g., Mitchum 1987; Morrissey 1990). The data period spans 30 years from 1958 to 1987. The original wind data in the chosen box have been edited so that daily means are not contaminated by unreasonably large values (e.g., 40 m s^{-1}). Because individual ship reports with values greater than 15 m s^{-1} are unlikely in the equatorial regions, they were checked with National Weather Service Pacific charts archived at the

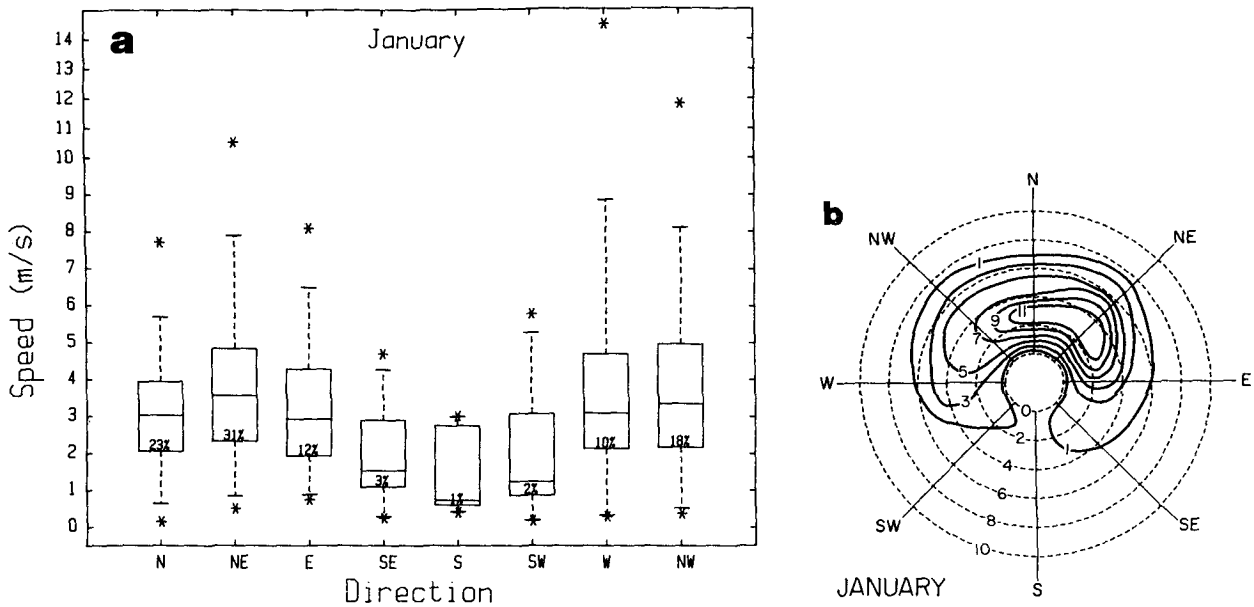

FIG. 4. (a) Modified box plots of daily surface wind in January 1958–87. The box shows the interquartile range extending from the lower quartile (p = 25%) to the upper quartile (p = 75%). The line through the box is the median, and the short horizontal line indicates the range where 95% of the data lies. The number in each box represents the percentage of wind in that particular direction (e.g., north) to the total number of observations in January. Extreme wind speeds are plotted as asterisks. (b) Frequency wind rose of daily surface wind in January 1958–87. Wind speeds (m s^{-1}) are denoted by values that lie along the dashed circles between S and SW. Frequencies (%) are contoured at 1, 3, 5, etc.

University of Hawaii; inconsistent reports have been deleted from the analyses.

3. Long-term climatology

a. Time series plots

Figure 2 shows the 3-day running mean of the zonal wind component, which fluctuates noticeably around the zero line. Easterly trade winds from the Northern and Southern hemispheres are predominant throughout the year in low latitudes. However, westerlies are not uncommon during some parts of the years shown in Fig. 2; the years characterized by strong westerly occurrences with mean wind speed greater than 7 m s^{-1} are 1961, 1963, 1972, 1979, 1981, and 1986. A comparably strong easterly component is observed in 1958, 1961, 1962, 1966, 1978, and 1984. As will be seen in section 5, ship observations are relatively few between 1958 and 1963. Thus, results of the zonal wind fluctuations in the early years are subject to some uncertainty.

Unlike the zonal wind component, the annual cycle of the meridional wind component is rather regular throughout the year (Fig. 3). In general, southerlies are observed from May to October and northerlies in the rest of the year. This feature is also apparent in Wyrtki and Meyers (1976) and Horel (1982), and mainly reflects the displacement of the monsoon trough during its annual course. Strong southerlies with speeds greater than 7 m s^{-1} are observed in 1961, 1972, 1974, and 1976. Based on monthly mean winds along the ship track over the western Pacific, Mitchum (1987) also noted the prevalence of strong southerlies in El Niño years. Another noteworthy feature in Fig. 3 is the presence of a persistently strong northerly component in late 1982 and early 1983. This, together with the increased easterly wind component observed during the same period (Fig. 2), suggests the strengthened northeast trades from the northwest Pacific at the peak of the 1982–83 ENSO. The northeasterly surges extend through the entire study domain and subsequently turn eastward due to the Coriolis force, forming a rather broad band of northwesterlies to the east of New Guinea (J. Sadler, personal communication).

b. Box plots and frequency wind roses

Variations of daily wind vectors from a large set of data are presented in modified box plots and frequency wind roses in this subsection. In this paper, we take a different approach from the conventional box plots (e.g., Graedel and Kleiner 1985). In the modified box plots, the interval where 95% of the data will lie is bounded by the broken line and only the most extreme values (the largest and the smallest) are plotted individually (e.g., Fig. 4a). Furthermore, the percentage of wind in any major direction is also provided. Because of rounding, the sum of the expected frequency of occurrence from all major wind directions does not necessarily equal 100%. In the following, diagrams will be presented only for the odd months (e.g., January, March, etc.).

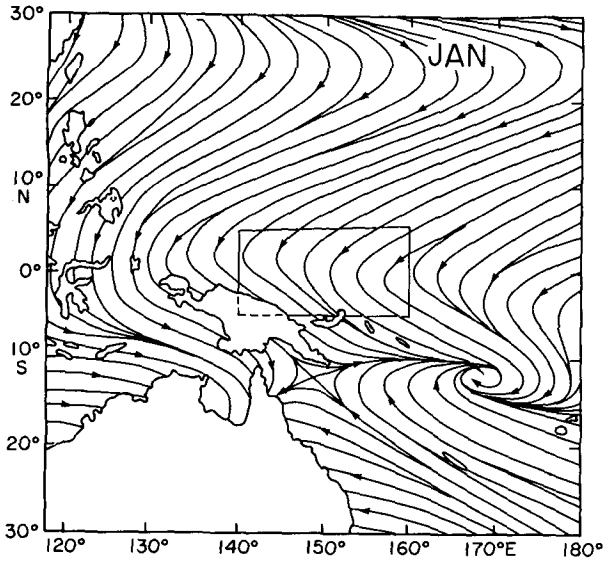

FIG. 5. Long-term January mean surface streamline analysis from COADS (after Sadler et al. 1987). The study domain is enclosed by a box.

As shown in Fig. 4a, northeasterlies and northerlies are most common in January, occurring 31% and 23% of the time, respectively. The occurrence of northwesterlies is also high (18%). Taken together, northeasterlies, northerlies, and northwesterlies account for 72% of the total number of observations in January (n = 857). Median wind speed is greatest (3.6 m s^{-1}) from the northeast and the highest wind speed is from the west (14.4 m s^{-1}). Westerly flows have the largest variability as 95% of the data lie in between 0.3 and 8.9 m s^{-1}, with a median speed of 3.1 m s^{-1}. The least likely wind directions in this month are southeasterlies, southerlies, and southwesterlies; the frequency distribution of wind speeds in these particular directions is positively skewed.

In concordance with the box plot, the frequency wind rose in January (Fig. 4b) exhibits that north to northeast winds, between 2 and 4 m s^{-1}, are most frequent. In the EWP, a strengthening of surface northerlies and northeasterlies often accompanies the penetrating cold surges from either east Asia or the northwest Pacific during boreal winter and spring (Lau and Chang 1987; Chu 1988). Thus, Fig. 4 simply reflects the predominance of the planetary-scale winter monsoon flows associated with the gigantic heat sink over the Asian continent. Climatologically, the monsoon trough over the Pacific is located near 12°S, just to the north of Australia, extending eastward from about 150°E to 170°E (Fig. 5). This configuration gives rise to northeasterly winds along the ship track north of the equator, northerlies at the equator, and northwesterlies south of the equator.

In March, northeasterlies, northerlies, and northwesterlies still prevail in the EWP, although their contribution has decreased somewhat to 62% collectively (Fig. 6a), as compared to January. The occurrence of easterlies has increased noticeably and the extremely high wind speed (12.3 m s^{-1}) comes from this direction. Westerlies are less likely to be observed in March than in January, and monsoon westerlies in March have a smaller range of variability than in January.

The frequency wind rose in March (Fig. 6b) is marked by a maximum contour in the northeast and east, with speeds between 2 and 4 m s^{-1}. Northerly

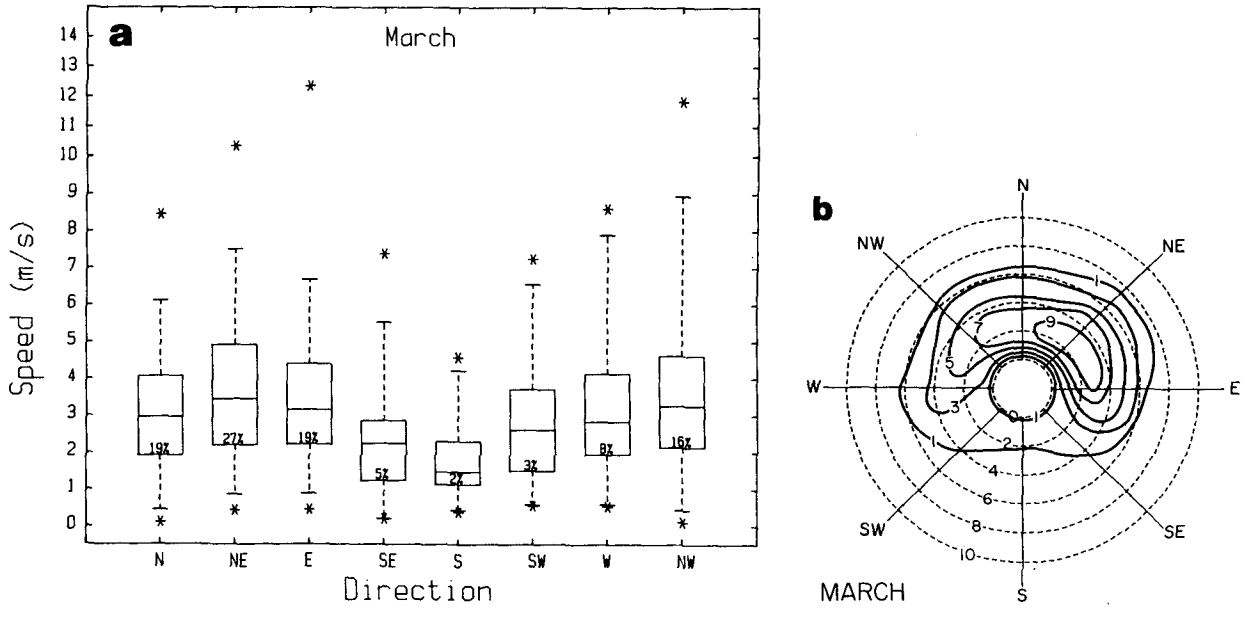

FIG. 6. Same as Fig. 4, but for March.

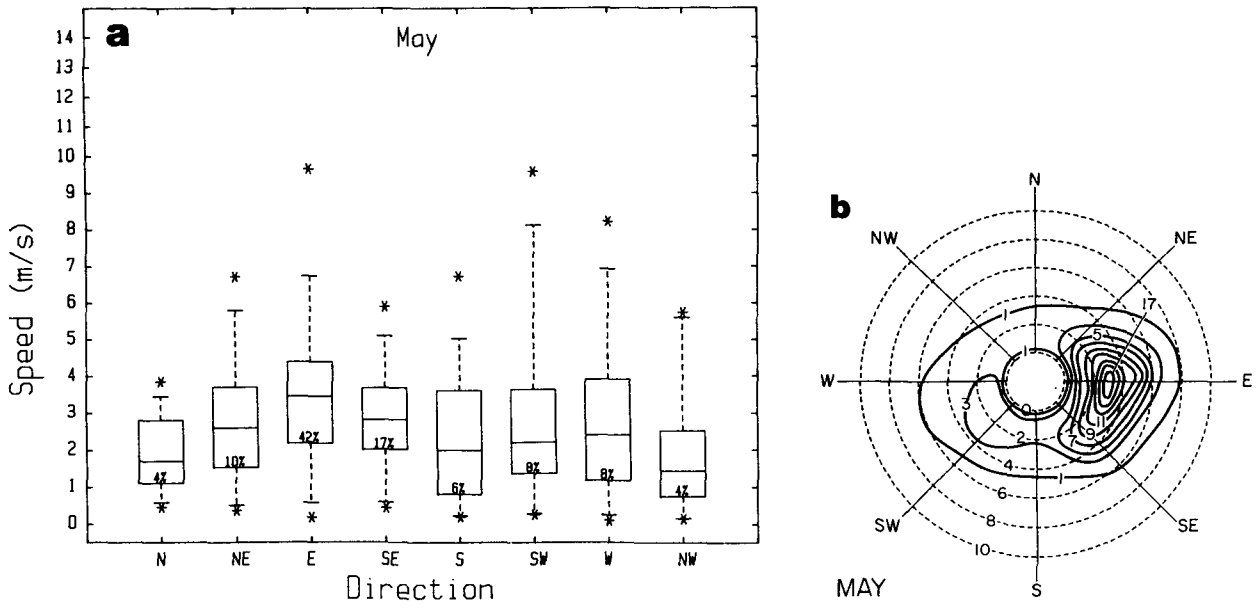

FIG. 7. Same as Fig. 4, but for May.

winds, with speed between 2 and 4 m s^{-1}, are also likely to be observed. In March, the winter monsoon of east Asia weakens, as does the Australian monsoon trough, which is then generally confined between 150°E and 160°E.

By May, easterlies reach their maximum frequency (42%), the highest in any single month (Fig. 7a). The largest median wind speed (3.5 m s^{-1}) and highest speed (9.7 m s^{-1}) also come from this direction. Southeasterlies rank second in the frequency of directions. The 95% range of variability in wind speed is highest for southwesterly winds, with a large extreme value (9.6 m s^{-1}). In May, the pattern of the wind rose has continued to shift toward the east (Fig. 7b). Easterlies between 2 and 4 m s^{-1} have more than a 17% frequency.

As the austral winter nears, southeast trades from the Southern Hemisphere begin to build up and reach a peak in July (30%, Fig. 8a). Easterlies and southerlies also become predominant as they occur 21% and 19% of the time, respectively. Winds from these three directions constitute 70% of the total number of obser-

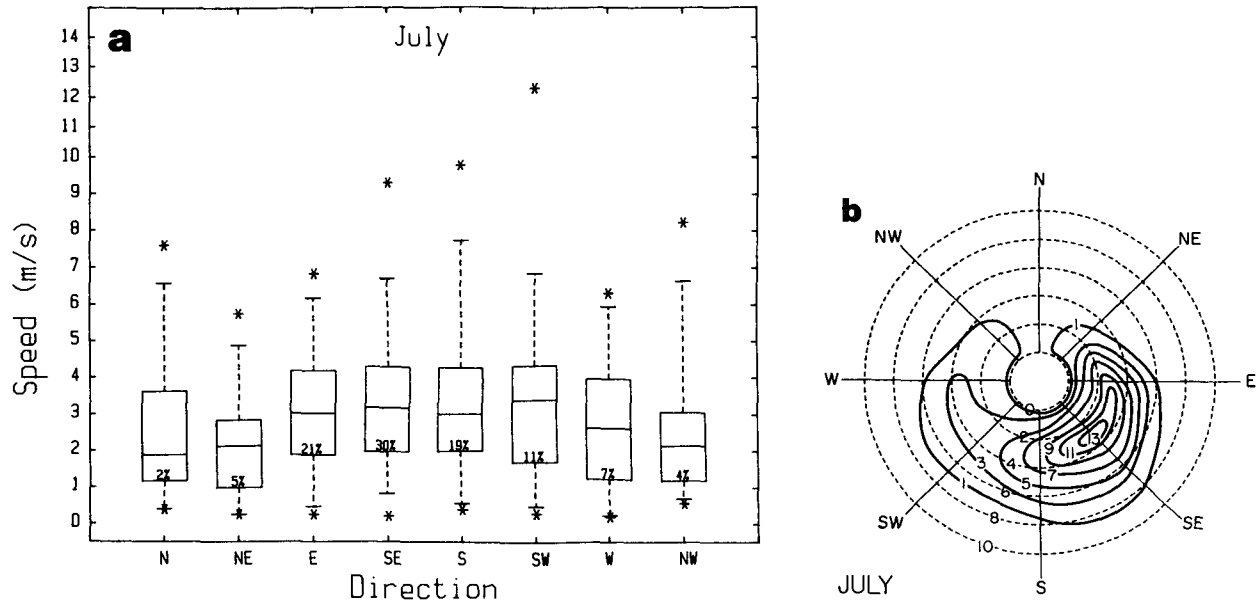

FIG. 8. Same as Fig. 4, but for July.

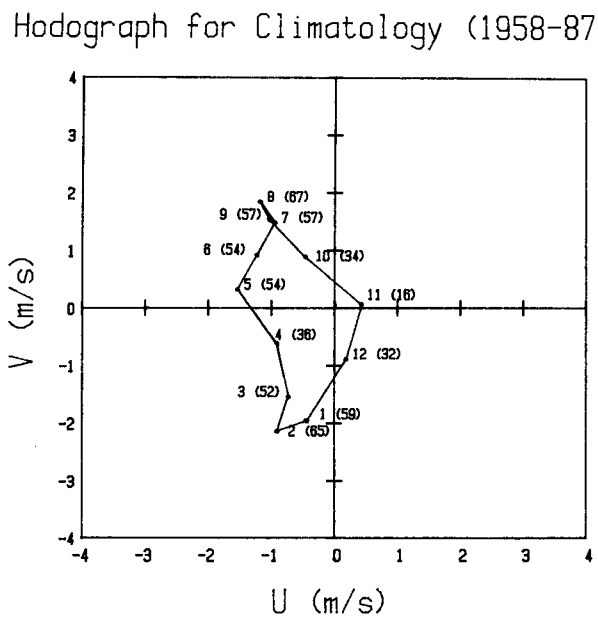

FIG. 13. Hodograph of long-term monthly mean wind vector from January to December. Number denotes month (e.g., 1 for January, etc). The value within parentheses indicates constancy in percentage.

preceding section will not be shown here. Figure 14 displays the frequency of occurrence for the eight major wind directions from November (−1) through December (0). November (−1), December (−1), and January (0) are generally regarded as the onset phase of an ENSO (e.g., Rasmusson and Carpenter 1982). To facilitate the comparison, Fig. 14 also presents the frequency of occurrence of climatological winds.

Since the onset of the 1982–83 ENSO came in the middle of the calendar year, rather than near December (−1), there is some concern whether this event should have been considered a typical pattern. In this regard, we have also produced another diagram by eliminating 1982 from the composite (not shown). Results from this new composite, however, do not show any apparent differences from Fig. 14, in which 1982 has been included. The difference in the frequency of occurrence of wind between the two composites is, on the average, about 1% to 2% from month to month. Therefore, the features presented in Fig. 14 are robust and should be representative of a canonical ENSO pattern.

In Fig. 14, northerlies tend to occur more frequently starting from January (0) and continuing toward May (0). Northwesterlies also increase their occurrence during the first half of the composite period, with large increases in February, March, and April (0). These features imply the enhanced influence of winter monsoons from the northwest Pacific at the early stage of ENSO.

Easterlies are less likely to be observed throughout the ENSO cycle (Fig. 14), and this reduction becomes conspicuous from January (0) until September (0). The larger decreases occur in April (14%), May (12%), June (12%), August (12%), and September (19%) of the ENSO year. Rasmusson and Carpenter (1982) also showed largest westerly anomalies in the EWP during August–October (0). Based on island wind data near the dateline, Harrison (1987) likewise demonstrated an increase in westerly anomalies at near-equatorial islands from May (0) to January (+1). In Fig. 14, a steady but small increase in the occurrence of westerlies is seen in almost all the months, varying from as small as 2% in January (0) to as large as 8% in May (0). Thus, reduced frequency in easterlies and increased frequency in westerlies indeed characterize surface winds during an ENSO year.

From June to September (0), at the peak of austral winter, southerlies and southwesterlies appear to occur more frequently. Mitchum (1987) also noted that the ENSO years (1965, 1972, 1976, and 1982) are marked by a strong southerly component in the Southern Hemisphere trade wind belts. This southerly wind component reached the equator in 1965 and even crossed the equator into the Northern Hemisphere in 1972 and 1982 (Mitchum 1987). Since the increased frequency of southerlies and southwesterlies occurs

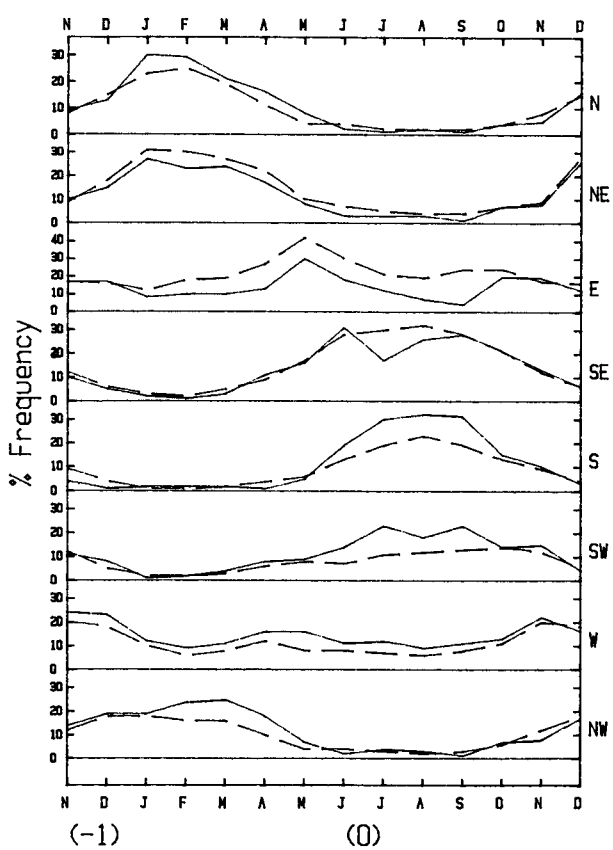

FIG. 14. Frequency of occurrence of the eight major wind directions plotted as a function of month through an ENSO cycle. Long-term climatology is denoted by the broken line.

from June to September (0), this occurrence is unique only at the later stage of ENSO, not at its early stage. This increased frequency may be interpreted as an atmospheric response to the anomalous heating in the equatorial Pacific after the onset of ENSO.

Figure 15 reveals the variations of the median wind speed from November (−1) through December (0), and the long-term climatology. During the early phase of an ENSO cycle, although northerlies and northwesterlies tend to occur more frequently (Fig. 14), the median wind speed of these two directions remains almost the same as the climatology (Fig. 15). Southerlies accelerate noticeably from June to September (0), consistent with the increased frequency of occurrence in southerlies during ENSO (Fig. 14). Strong southwesterlies occur only intermittently, in December (−1), January (0), and May (0). Because there are very few observations of southwesterlies in January (0) (Fig. 14), the interpretation of their strength in that month is subject to some uncertainty (Fig. 15).

Easterlies occur not only less frequently but also with reduced strength during an ENSO cycle (Figs. 14 and 15). Stronger westerlies are observed in most months, particularly in November (−1) and in May and June (0). By comparing the fluctuations of easterlies and westerlies, one notes that, in general, the reduction in strength of easterlies is more pronounced than the corresponding increase of westerlies. Thus, the large westerly anomalies, for example, during August–October (0) in Rasmusson and Carpenter (1982, their Fig. 20), are probably indicative of the reduced easterlies in the EWP, rather than a sequence of westerly wind bursts. However, the impulsive decrease in equatorial easterlies, according to linear theory (e.g., Cane and Sarachik 1981), may have the same effect on the tropical ocean as westerly wind bursts.

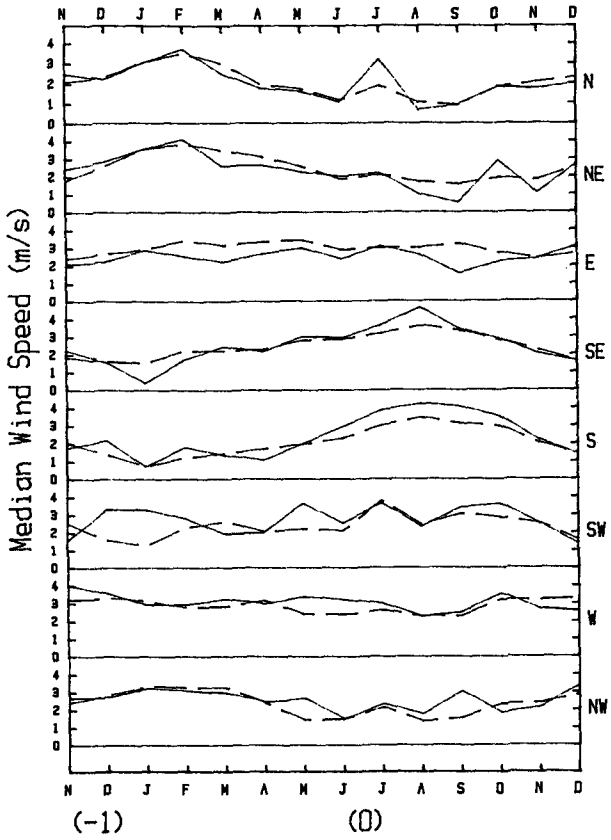

FIG. 15. Median wind speed from the eight major wind directions plotted as a function of month through an ENSO cycle (solid). Median wind speed from the long-term climatology is denoted by the broken line.

b. Monte Carlo simulation

As described in the preceding subsection, the frequency of occurrence of surface wind during the ENSO composite in some months is very different from the climatology. Now the natural question arises as to whether other randomly selected composites could have produced the same kind of statistic as the ENSO composite. A null hypothesis is therefore established that the frequency of occurrence during the ENSO composite (six events) is equivalent to a wind sample randomly formed from the 30-year record.

In the Monte Carlo simulation, the 30-year record is scrambled into a group of six years using a random number generator. This procedure is then repeated in a very large number of trials. According to Noreen (1989), the significance level of the test is $(ng + 1)/(N + 1)$, where ng is the number of simulated samples for which the values of the test statistic is at least as large as the test statistic for the ENSO composite, and N is the number of simulated random samples. In our case, N is 999 and the test statistic is the frequency of occurrence of wind. Livezey and Chen (1983) discussed another application of Monte Carlo simulation as applied to assessing the field significance.

Table 1 lists the significance level of the simulation for the eight major wind directions through an ENSO cycle. For northerlies in April and May, the probability of obtaining a test statistic as large as that observed during an ENSO cycle is about 5% in a random size of 999. For northwesterlies in February, March, and April, the chance of getting a value from the random sample comparable to the corresponding ENSO statistics is extremely low, ranging from 0.5% to 3.6%. This is also true for southerlies and southwesterlies from June to September. For easterlies, the low probability occurs consecutively from March to September, indicating that the reduced frequency of occurrence of easterlies during an ENSO cycle could not have occurred by random chance. In contrast, the increased occurrence of westerlies only becomes statistically significant in May.

c. Hodograph of monthly mean wind vectors

Figure 16 shows the variations of the monthly mean vector of the surface winds and the corresponding con-

stancy during an ENSO cycle. Northwesterly flows prevail in November and December (−1), and northerly flows dominate the EWP from January to April (0). As compared to the climatology (Fig. 13), easterlies in Fig. 16 have reduced their strength noticeably from January to October (0). This is consistent with the weakening of the Pacific Walker circulation during the 1982–83 ENSO as the major convection area migrates eastward from the Indonesian maritime continent to the equatorial central Pacific (e.g., Lau and Chang 1987). However, decreased surface easterlies in the EWP should not be directly interpreted as a decrease in the strength of the Walker circulation. Since the Walker circulation is a thermally forced zonal cell with rising motion over the warm western Pacific and subsidence over the cold eastern Pacific, a change in the zonal distribution of heating anomalies would be a better measure of the Walker cell intensity than a change in the surface wind field.

The wind vector in November (0) resembles the climatology, and in December (0) it is mainly northerly. Another feature of interest in Fig. 16 is the predominance of the strong southerly wind component from June to September (0). The constancy of the wind is below 30% in November (−1), April, May, and November (0). However, compared with the climatology, the wind fluctuations become more stable in November (−1) and November (0). A high steadiness of wind (≥60%) occurs in two different periods: namely, from January to February (0), and from July to September (0).

5. Some statistics of westerly wind events

In this section, some important statistical features of westerly wind events are presented. Emphasis is placed on the following issues: how often westerly wind events occur, how long they last, what are the location and scale parameters that typify different kind of events, and what changes there are in the aforementioned statistics during the El Niño years. The issue of spatial extent of westerly wind patterns cannot be addressed in this study, because areal-averaged data are used. However, based on our previous case studies, westerly events are generally confined to within five degrees of the equator (Chu 1988; Chu and Frederick 1990). The zonal domain covered by the westerly wind events, though, can vary considerably, from about 1000 km to 3500 km. Westerly events are referred to here as episodes of nonnegative zonal wind anomalies ($u' \geq 0$) for at least five or more consecutive days, a threshold period regarded as having effects on the eastern Pacific Ocean (Giese and Harrison 1990). In their work, the wind forcing is modeled according to a Gaussian function with a duration at half-amplitude of about five days. Harrison and Giese (1991) also found this typical time scale in their composite chart when the observed westerly anomalies were centered along the equator near the dateline. In this study, anomalies are the difference between individual daily value and the daily median value.

a. Climatology

Figure 17a shows the time series of the total annual number of westerly wind anomalies (WWA) from 1958 through 1987. Except for the recent two ENSO events, the number of WWA is high during ENSO years, such as 1965, 1969, 1972, and 1976. Also notable in Fig. 17a is the rather small interannual variations from 1958 to 1964, probably as a result of relatively few ship observations in the early years (Fig. 17b).

In the following, the duration of WWA is categorized into six groups. Category one is assigned to the case when five to seven consecutive days of WWA are observed, category two is the case when eight to ten consecutive days of WWA are observed, and so on. Accordingly, category six is the case when more than 20

TABLE 1. The probability of falsely rejecting the null hypothesis in $N = 999$ Monte Carlo trials as a function of wind direction and the month through an ENSO cycle. The numbers in italics exceed the conventional 5% significance level.

	Wind octant							
	N	NE	E	SE	S	SW	W	NW
Nov (−1)	0.454	0.279	0.484	0.283	***0.027***	0.405	0.181	0.333
Dec (−1)	0.385	0.225	0.493	0.347	***0.025***	0.129	0.193	0.304
Jan (0)	0.075	0.288	0.129	0.253	0.298	0.199	0.248	0.378
Feb (0)	0.205	0.121	0.097	0.134	0.310	0.477	0.103	***0.005***
Mar (0)	0.312	0.291	***0.014***	0.192	0.390	0.341	0.157	***0.036***
Apr (0)	0.053	0.175	***0.021***	0.227	0.054	0.179	0.128	***0.010***
May (0)	***0.046***	0.302	0.054	0.424	0.399	0.333	***0.020***	0.056
Jun (0)	0.100	***0.038***	***0.030***	0.318	***0.014***	***0.012***	0.095	0.068
Jul (0)	0.080	0.053	***0.046***	***0.005***	***0.015***	***0.004***	0.068	0.397
Aug (0)	0.330	0.255	***0.017***	0.128	***0.029***	***0.042***	0.109	0.174
Sep (0)	0.238	***0.011***	***0.001***	0.478	***0.013***	***0.009***	0.223	0.078
Oct (0)	0.432	0.368	0.327	0.461	0.231	0.466	0.320	0.315
Nov (0)	0.086	0.380	0.234	0.308	0.370	0.147	0.394	***0.046***
Dec (0)	0.354	***0.035***	0.195	0.475	0.270	0.284	0.366	0.423

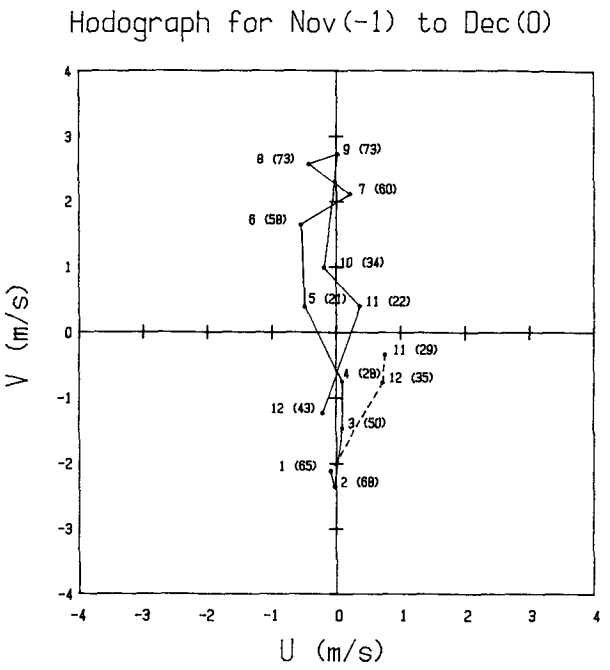

FIG. 16. Hodograph of monthly mean wind vector through an ENSO cycle. Solid line is for the ENSO year and broken line is November and December of the antecedent year. The value in the parenthesis indicates constancy in percentage.

consecutive days of WWA have occurred, a rare event that is only 3% of all six categories. The choice of a three-day span of duration for each category in the classification (except category 6) is considered so that the number of cases in each category is neither too small to cause irregular fluctuations nor too large to exhibit featureless patterns. Figure 18 shows the modified box plot of WWA for six different categories. Regardless of whether the duration of WWA is short or long, the median wind speed for the six categories varies little, from 1.84 m s^{-1} in category one to 2.79 m s^{-1} in category six. The highest wind speed (14.53 m s^{-1}) among all six categories is from category one: namely, five to seven days of westerly anomalies. Category five (i.e., 17 to 19 days of WWA) has the largest variability as 95% of the anomalies lie in between 0.06 and 8.83 m s^{-1}.

In terms of the frequency of occurrence, category one has the highest frequency (61%), suggesting the prevalence of a synoptic nature of WWA in the western Pacific warm pool region (Fig. 18). It is also notable that the first three categories account for 87% of the total number of observations. Hence, westerly events, once formed, generally will not last for more than 13 days. For the first three categories of WWA, the months with a relative low number of occurrences are April and May, and the months with a relative high number of occurrences are October, November, and December (Table 2). When WWA have a duration equal to or longer than 14 days, they occur more frequently in April and May. If we include all six categories together, the total number of WWA does not vary much throughout the year, although a relative maximum is still found in October (the peak), November, and December.

b. El Niño years

Based on the six El Niño years identified earlier (i.e., 1965, 1969, 1972, 1976, 1982, and 1987), the descriptive statistics of WWA for six categories are illustrated in Fig. 19. As compared to the climatology (Fig. 18), the median wind speed of WWA tends to increase slightly during the El Niño years, and this increase is more pronounced for categories two, four, and five (Fig. 19). During the El Niño years, there is a substantial reduction in the frequency of occurrence from the climatology for the first category (17%). Thus, WWA with 5 to 7 days duration, although still the leading category among all six, are observed less during the El Niño years. In contrast, there is an increase in

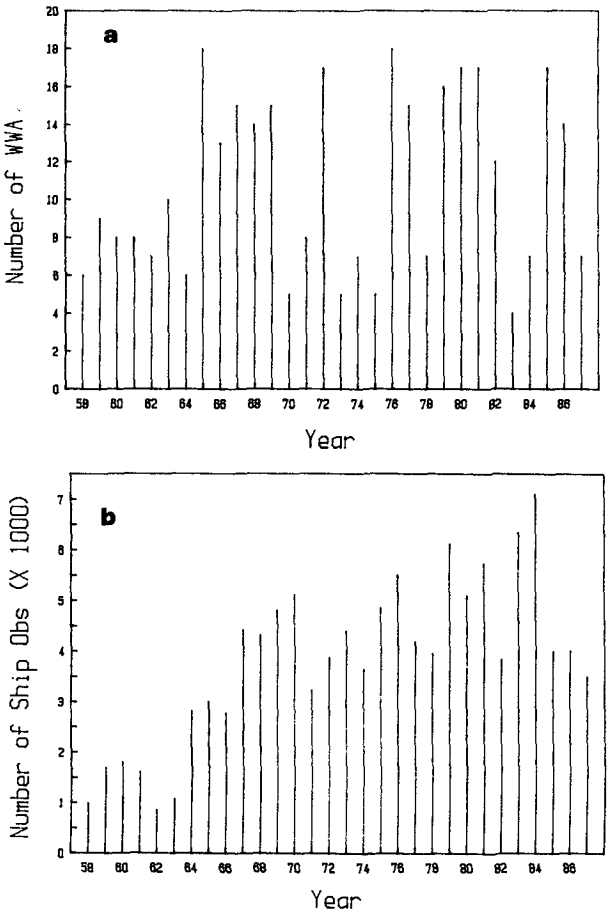

FIG. 17. (a) Time series of the number of annual westerly wind anomalies in the equatorial western Pacific from 1958 to 1987. (b) Time series of the number of annual ship observations in the equatorial western Pacific from 1958 to 1987.

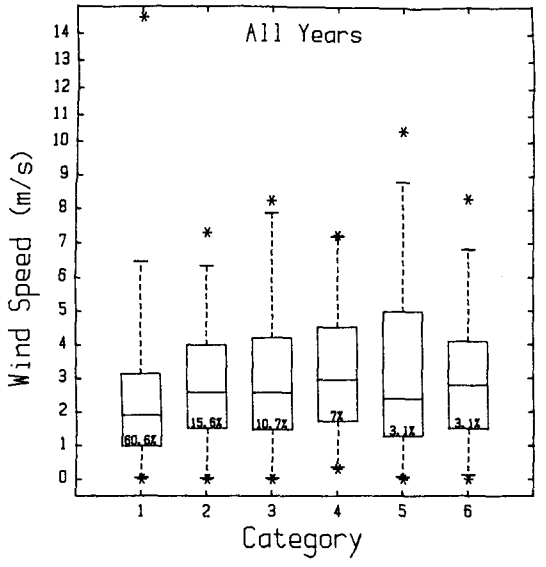

FIG. 18. Westerly wind anomalies (WWA) from 1958 to 1987. The box shows the interquartile range extending from the lower quartile ($p = 25\%$) to the upper quartile ($p = 75\%$). The line through the box is the median, and the short horizontal line indicates the range where 95% of the data lies. The number in each box represents the percentage of WWA in that particular category to the total categories. Categories and WWA periods, respectively, are: one, 5 to 7 days; two, 8 to 10 days; three, 11 to 13 days; four, 14 to 16 days, five, 17 to 19 days; six, 20 days and more.

the frequency of occurrence for the other five categories; in particular, a 6% increase for category two and 6.5% for category three. Hence, westerly wind anomalies in the EWP with a duration longer than 7 days, particularly between 8 and 13 days, tend to occur more often during El Niño years. It is thus possible that such an effect would produce more significant oceanographic response in the eastern Pacific than the case with westerly anomalies of very short duration.

6. Summary and conclusions

Because monthly data often mask the nature of variability of surface winds in the equatorial waveguide, exploratory analysis is used to provide information regarding the statistical properties of daily wind along a ship track in the equatorial western Pacific. This is a region in which the intermittent synoptic-scale wind bursts may play an important role in the initiation and maintenance of El Niño and data are relatively abundant for statistical analyses. In fact, this is the only equatorial region west of 175°E where historical observations are available. To summarize the wind characteristics, the modified box plots, frequency wind roses, and a hodograph of wind vectors are used. Results obtained from these methods complement the existing atlases (e.g., Wyrtki and Meyers 1975; Sadler et al. 1987) by providing more detailed information. These include the expected frequency of occurrence of wind from a particular wind direction, the intensity

TABLE 2. Number of westerly wind anomalies throughout the annual cycle from 1958 to 1987.

	Total number	Number in categories 1, 2, and 3 (i.e., 5 to 13 days)	Number in categories 4, 5, and 6 (i.e., 14 days and above)
Jan	24	20	4
Feb	25	23	2
Mar	27	24	3
Apr	25	18	7
May	27	19	8
Jun	26	25	1
Jul	24	22	2
Aug	27	24	3
Sep	28	26	2
Oct	33	33	0
Nov	30	28	2
Dec	31	29	2

(i.e., median) and the range of variability of the speed for a particular direction (i.e., interquartile range), and the steadiness of wind.

Based on the recent 30-year record (1958–87), the box plots exhibit that the prevailing wind in the EWP region veers successively from north-northeast in January to east-southeast in September. This shift is also very clear in the frequency wind roses and is consistent with previous analyses (e.g., Wyrtki and Meyers 1976; Horel 1982). Specifically, northeasterly, northerly, and northwesterly monsoonal flows dominate the period from December to April. Southeast trades, southerly, and southwesterly flows cross the equator from May to October. Easterlies are common throughout the year, peaking in May (42%). Thus, the deep equatorial re-

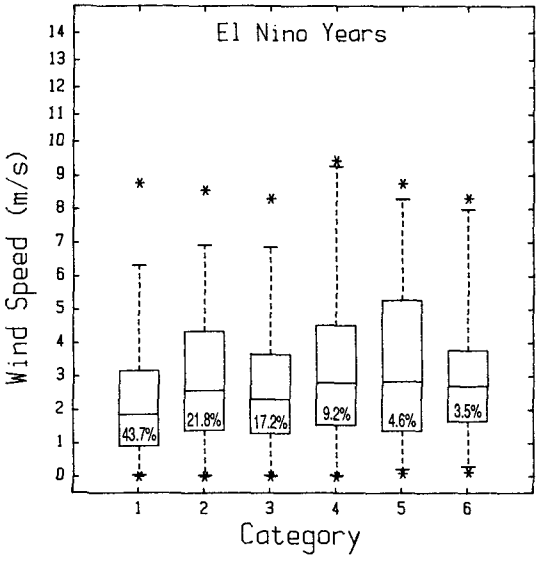

FIG. 19. Same as Fig. 18, except for El Niño years.

gion is influenced by trade winds from each winter hemisphere, and by the eastern Pacific subtropical anticyclones during the transition seasons (i.e., May or October). Equatorial westerlies reach their peak in November (20%) and December (18%), with a secondary peak in April (11%). However, the extremely low steadiness of the wind in November implies that the double near-equatorial monsoon trough, as revealed in the climatic atlases (Fig. 12), is not a quasi-stationary circulation system and may be subject to noticeable changes from year to year. This feature has not been recognized before.

Wind data are further composited according to the ENSO cycle. A higher number of occurrence of northerlies and northwesterlies is observed from January to May (0) in the boreal winter and spring. As the season progresses to the austral winter [from June to September (0)], there is an increased occurrence of southerlies and southwesterlies. These increased occurrences of wind during an ENSO cycle, particularly southerlies and southwesterlies, are unusual relative to those generated from a large random sample by the Monte Carlo technique. Thus, these cross-equatorial flows are statistically significant at the 5% level.

As expected, westerlies increase their frequency of occurrence during an ENSO cycle; this increase is most pronounced in December (−1), April (0), May (0), and July (0), with the increase in these months being at least 5%. Only in May (0) is the increase statistically significant. On the other hand, there is a substantial decrease in the frequency of occurrence in easterlies from January to September (0), with the amount being as large as 19% in September (0). This large decrease is extremely unusual relative to the simulated samples and thus it could not have occurred by random chance. Loosely speaking, monsoon westerlies tend to be stronger and equatorial easterlies weaker during an ENSO cycle. The net change of the zonal wind fluctuations from November (−1) to February (0) is less than, say, the net change from March to June (0) in the frequency of occurrence (Fig. 14). The net change during the latter period is mainly due to the decrease of easterlies, and this decrease would result in the same dynamic effect, in the framework of linear numerical models, as the westerly bursts.

Events of westerly wind anomalies are stratified in six categories in terms of their temporal variations. Most events are of category one (61%), with a duration around 5 to 7 days. This kind of westerly anomaly, together with the next two categories (i.e., 8 to 13 days duration), occurs most frequently in October, November, and December. During El Niño years, the frequency of occurrence of category one is reduced markedly while the frequency of occurrence of other categories with a longer duration is increased. Using an ocean circulation model with an idealized wind patch, Giese and Harrison (1990) demonstrated that a single 10-day episode of remote wind forcing can result in more than two months of warming near the South American coast. They further suggested that a sequence of westerly anomalies, when occurring in a close time interval, could reproduce the surface warming patterns as seen during ENSO. Since the strength of the wind forcing can be specified as a function of the time scale of the wind patch (Giese and Harrison 1990), it is not unreasonable to surmise that the longer duration ($\geq$8 days) of the westerly anomalies observed during the ENSO composite may excite equatorially trapped Kelvin waves more energetically and maintain the anomalously warm surface water in the eastern Pacific.

The aforementioned temporal variation and preferred timing of occurrence of westerly wind anomalies may provide some useful information on maximizing efforts and deployments of various platforms and instruments for the proposed field experiment of the Tropical Ocean and Global Atmosphere (TOGA) program: namely, the Coupled Ocean–Atmosphere Response Experiment (COARE). The Intensive Observation Period (IOP) of the TOGA-COARE is scheduled to be conducted from November 1992 through February 1993 in the tropical western Pacific warm pool region. Furthermore, since the peak month of westerly wind anomalies is October and one of the main objectives of the TOGA-COARE is to study air–sea interaction associated with events of westerly wind anomalies, it seems that October 1992 should be considered to be included in the proposed field experiment as well.

Acknowledgments. We acknowledge the assistance of A. Hori and M. Morrissey in retrieving the individual marine reports from COADS and interim COADS, and L. Oda in drafting some of the figures. G. Mitchum commented on an early version of this paper. We are also grateful to Eugene Rasmusson, Peter Lamb, and an anonymous official reviewer whose comments helped greatly to improve this paper. This study is partially supported by NOAA Equatorial Pacific Ocean Climate Studies program (NA-85-ABH-00032) and USDA Contract PSW-90-0001CA.

REFERENCES

Cane, M. A., and E. S. Sarachik, 1981: The response of a baroclinic equatorial ocean to periodic forcing: The linear periodic case. *J. Mar. Res.*, **39**, 651–693.

Chu, P.-S., 1988: Extratropical forcing and the burst of equatorial westerlies in the western Pacific: A synoptic study. *J. Meteor. Soc., Japan.*, **66**, 549–564.

——, and J. Frederick, 1990: Westerly wind bursts and surface heat fluxes in the equatorial western Pacific in May 1982. *J. Meteor. Soc., Japan.*, **68**, 523–537.

Giese, B. S., and D. E. Harrison, 1990: Aspects of the Kelvin wave response to episodic wind forcing. *J. Geophys. Res.*, **95**(C5), 7289–7312.

Gill, A. E., 1982: *Atmosphere-Ocean Dynamics.* Academic Press, 662 pp.

Graedel, T. E., and B. Kleiner, 1985: Exploratory analysis of atmospheric data. *Probability, Statistics, and Decision Making in the*

Atmospheric Sciences, A. H. Murphy and R. W. Katz, Eds., Westview Press, 1–43.

Harrison, D. E., 1987: Monthly mean island surface winds in the central Pacific and El Niño events. *Mon. Wea. Rev.*, **115,** 3133–3145.

——, and D. S. Luther, 1990: Surface winds from tropical Pacific islands—climatological statistics. *J. Climate,* **3,** 251–271.

——, and B. S. Giese, 1991: Episodes of surface westerly winds as observed from islands in the western tropical Pacific. *J. Geophys. Res.*, **96**(Suppl), 3221–3237.

Horel, J. D., 1982: On the annual cycle of the tropical Pacific atmosphere and ocean. *Mon. Wea. Rev.*, **110,** 1863–1878.

Keen, R. A., 1988: Equatorial westerlies and the Southern Oscillation. *Proc. of the U.S. TOGA Workshop on Western Pacific Air–Sea Interaction,* R. Lukas and P. Webster, Eds., U.S. TOGA Report 8, UCAR, Boulder, 121–140.

Lander, M., 1989: A comparative analysis of the 1987 ENSO event. *Trop. Ocean–Atmos. Newslett.*, **49,** 3–6.

Lau, K.-M., and C.-P. Chang, 1987: Planetary scale aspects of the winter monsoon and atmospheric teleconnections. *Monsoon Meteorology,* C.-P. Chang, and T. N. Krishnamurti, Eds., Oxford University Press, 161–202.

——, P. Li, C. H. Sui and T. Nakazawa, 1989: Dynamics of super cloud clusters, westerly wind bursts, 30–60 day oscillations and ENSO: An unified view. *J. Meteor. Soc. Japan.*, **67,** 205–219.

Livezey, R. E., and W. Y. Chen, 1983: Statistical field significance and its determination by Monte Carlo techniques. *Mon. Wea. Rev.*, **111,** 46–59.

Lukas, R., S. P. Hayes, and K. Wyrtki, 1984: Equatorial sea-level response during the 1982–83 El Niño. *J. Geophys. Res.*, **C6**(10), 425–430.

Luther, D. S., and D. E. Harrison, 1984: Observing long-period fluctuations of surface winds in the tropical Pacific: Initial results from island data. *Mon. Wea. Rev.*, **112,** 285–302.

——, D. E. Harrison and R. A. Knox, 1983: Zonal winds in the central equatorial Pacific and the onset of El Niño. *Science,* **222,** 327–330.

Madden, R., and P. Julian, 1972: Description of global-scale circulation cells in the tropics with a 40–50 day period. *J. Atmos. Sci.*, **29,** 1109–1123.

McPhaden, M. J., H. P. Freitag, S. P. Hayes, B. A. Taft, Z. Chen, and K. Wyrtki, 1988: The response of the equatorial Pacific Ocean to a westerly wind burst. *J. Geophys. Res.*, **C9**(93), 10 589–10 603.

Mitchum, G. T., 1987: Trade wind fluctuations associated with El Niño-Southern Oscillation. *J. Geophys. Res.*, **C9**(92), 9464–9468.

Morrissey, M. L., 1990: An evaluation of ship data in the equatorial western Pacific. *J. Climate,* **3,** 99–112.

Nakazawa, T., 1988: Tropical super clusters within intraseasonal variations over the western Pacific. *J. Meteor. Soc. Japan.*, **66,** 823–839.

Nitta, T., 1989: Development of a twin cyclone and westerly bursts during the initial phase of the 1986–87 El Niño. *J. Meteor. Soc. Japan.*, **67,** 677–681.

Noreen, E. W., 1989: *Computer Intensive Methods for Testing Hypotheses.* John Wiley and Sons, 229 pp.

Rasmusson, E. M., and T. H. Carpenter, 1982: Variations in tropical sea surface temperature and surface wind fields associated with the Southern Oscillation/El Niño. *Mon. Wea. Rev.*, **110,** 354–384.

Sadler, J., M. Lander, A. Hori, and L. Oda, 1987: Tropical marine climatic atlas. UHMET Rep. 87-02, Dept. of Meteorology, University of Hawaii, Honolulu, 26 pp.

Wyrtki, K., and G. Meyers, 1975: The trade wind field over the Pacific Ocean, Part 1: The mean field and the mean annual variation. Hawaii Institute of Geophysics, Rep. HIG-75-1, 25 pp.

——, and ——, 1976: The trade wind field over the Pacific Ocean. *J. Appl. Meteor.*, **15,** 698–704.